Article:

Ma, CY orcid.org/0000-0002-4576-7411 and Roberts, KJ orcid.org/0000-0002-1070-7435 (2018) Combining Morphological Population Balances with Face-Specific Growth Kinetics Data to Model and Predict the Crystallization Processes for Ibuprofen. Industrial and Engineering Chemistry Research, 57 (48). pp. 16379-16394. ISSN 0888-5885

https://doi.org/10.1021/acs.iecr.8b02140

Combining Morphological Population Balances with Face-Specific Growth Kinetics Data to Model and Predict the Crystallisation Processes for Ibuprofen

C. Y. Ma and K. J. Roberts

Centre for the Digital Design of Drug Products, School of Chemical and Process Engineering, University of Leeds, Leeds, LS2 9JT, United Kingdom

Corresponding author:
Dr Cai Yun Ma
School of Chemical and Process Engineering
University of Leeds
Leeds LS2 9JT
UK
Tel +44 113 343 7809
Email c.y.ma@leeds.ac.uk

Abstract

A route map for modelling pharmaceutical manufacturing processes utilising morphological population balance (MPB) is presented in terms of understanding and controlling of particle shape and size for optimising the efficiency of both the manufacturing process and final properties of the formulated drugs. This is applied to batch cooling crystallisation of the pharmaceutical compound, ibuprofen, from supersaturated ethanolic solutions in which the MPB is combined the known crystal morphology and associated face-specific growth kinetics (Nguyen et al., CrystEngComm, 2014, 16, 4568-4586) to predict the temporal evolution of the shape and size distributions of all crystals. The MPB simulations capture the temporal evolution of the size and shape of ibuprofen crystals and their distributions at each time instance during the crystallisation processes. The volume equivalent spherical diameter and crystal size distribution converted from MPB simulation are validated against the experimentally studies on the 1 litre scale size (Rashid et al., Chem Eng Res & Des, 2012, 90, 158-161), confirming the promise of this approach as a powerful simulation, optimisation and control tool for the digital design of precision pharmaceutical processes and products with the desirable properties, with potential applications in crystallisation design for personalised medicines.

Keywords: Morphological Population Balance (MPB), Pharmaceutical Manufacture, Morphological Modelling, Batch Crystallisation, Ethanolic Solutions, Crystal Shape Distribution, Crystal Size Distribution, Ibuprofen

1. INTRODUCTION

A typical pharmaceutical manufacturing process for solid form drug products comprises primary stage whereby the target active pharmaceutical ingredient (API) is synthesised and crystallised into a highly crystalline product of high purity. This is then subsequently formulated through the addition of excipients via a number of secondary processing stages (filtration, drying, milling, blending, granulation, compaction and tableting) to produce practical dosage forms containing various API strengths (Figure 1). The overall life cycle of drug particles spans from solute to primary and secondary processes, then dissolution process for efficient drug delivery to patients. When the pharmaceutical materials progress through these manufacturing/delivery processes, they can be subject to phase changes (crystallisation or dissolution) and often particle size/shape modifications due to the mechanical action of the different unit operations. Therefore, it is important to predict, optimise and control the performance and interconnectivity of the unit operations involved in the overall processes flow diagram with the aim to produce the desired final products and the performance of drug delivery. The schematic (Figure 1) and accompanying narrative highlight the complexity of the manufacturing chain for pharmaceuticals. Although this study focuses on crystallisation processes, the modelling methodology is quite applicable to the other unit operations used in drug manufacture. For example, inter-crystal aggregation is important in the blending, granulation and compaction processes.

Population balance (PB) modelling (for example[1-10]) has proved to be an excellent simulation tool for predicting the evolution of crystal size distributions for many practical processes. However, crystalline materials in their processing environment are inherently rarely spherical in terms of their external particle morphology. Indeed their inherent crystallographic structural motifs gives rise to a polyhedral morphologies with each crystal face {hkl} displaying different surface chemistry and hence different physical and chemical properties. Hence, to effectively simulate such systems, full consideration of both particle size and shape is an obvious pre-requisite. The particle manufacturing industries, in particular, pharmaceuticals and fine chemicals, need to predict and control both size and shape distributions of crystalline products and hence the capability of PB models has recently been extended to encompass the crystal shape anisotropy. This has been done by directly integrating the crystal morphological related information (indexed morphology plus face-specific growth kinetics) with PB for designing the manufacture of high purity crystals which have the desirable size and shape distributions and also the desirable surface properties of individual faces, i.e., a morphological population balance (MPB) model[11-20]. MPB models are formulated based upon particle number density conservation and involve a population of particles which undergo changes in size and shape during processing. The well-established morphology prediction tools for single crystals, such as

HABIT[21, 22], can provide the exact crystal shape and , based on this, MPB models can be developed according to the growth rates of the individual crystal faces and their normal distances from the crystal centre[11].

For different unit operations during the pharmaceutical manufacture processes, the MPB models may include a few or all of the following terms, nucleation kinetics, faceted crystal growth mechanisms, faceted agglomeration and breakage kernels (Figure 1), which directly controls the final size/shape distributions. For primary processes, all of the four terms can be important, but overall faceted crystal growth can be expected to be more dominant. For secondary processes, the face-specific agglomeration and breakage can also be important, in particular when the processes do not involve in high amount of solvents or binders. For dissolution process, the de-aggregation, de-agglomeration and face-specific dissolution mechanisms can control the effective and accurate release of API for precision drug delivery. Furthermore, the MPB models can be used for well-mixed systems and also hydrodynamic systems having inhomogeneous property distribution in the manufacturing units via either multi-zonal modelling techniques (e.g. [23-25]) or fully coupling methods[23, 26, 27].

In this paper, the development and application of MPB modelling methodology for pharmaceutical crystallisation processes is presented as a key component of an overall process route map based upon the first-principles predictive models that can be used for the digital design and control of pharmaceutical manufacturing processes[28] and, through this, for the more effective and personalised delivery of medicines to patients. Its relevance to pharmaceutical processes is highlighted through the application to crystallisation processes integrating crystal morphology and growth kinetics with the population balance through the MPB. Despite some studies[11, 12, 14, 16-18, 24, 29, 30] employing MPB method (or similar concept) to simulate crystal shape/size, only a few of them have applied MPB to organic materials. A new search method is developed to systematically search the face-based crystal size distribution (CSD) space with multiple parameters based on the volume-equivalent experimental data, hence obtaining face-based seeds size distributions and facet growth rates for MPB simulation. This study is also the first to fully integrate the face specific {hkl} growth rate data into the MPB including the incorporation of the effect of both interface kinetics and mass transfer on the growth rates and face-specific mechanisms. The MPB application to pharmaceutical crystallisation processes is illustrated through a case study of ibuprofen crystallised from ethanol in seeded batch crystallisers to predict the evolution of crystal shape/size distributions and compare with measurements. To our knowledge, this is also the first attempt to validate MPB simulation results against experimentally determined data.

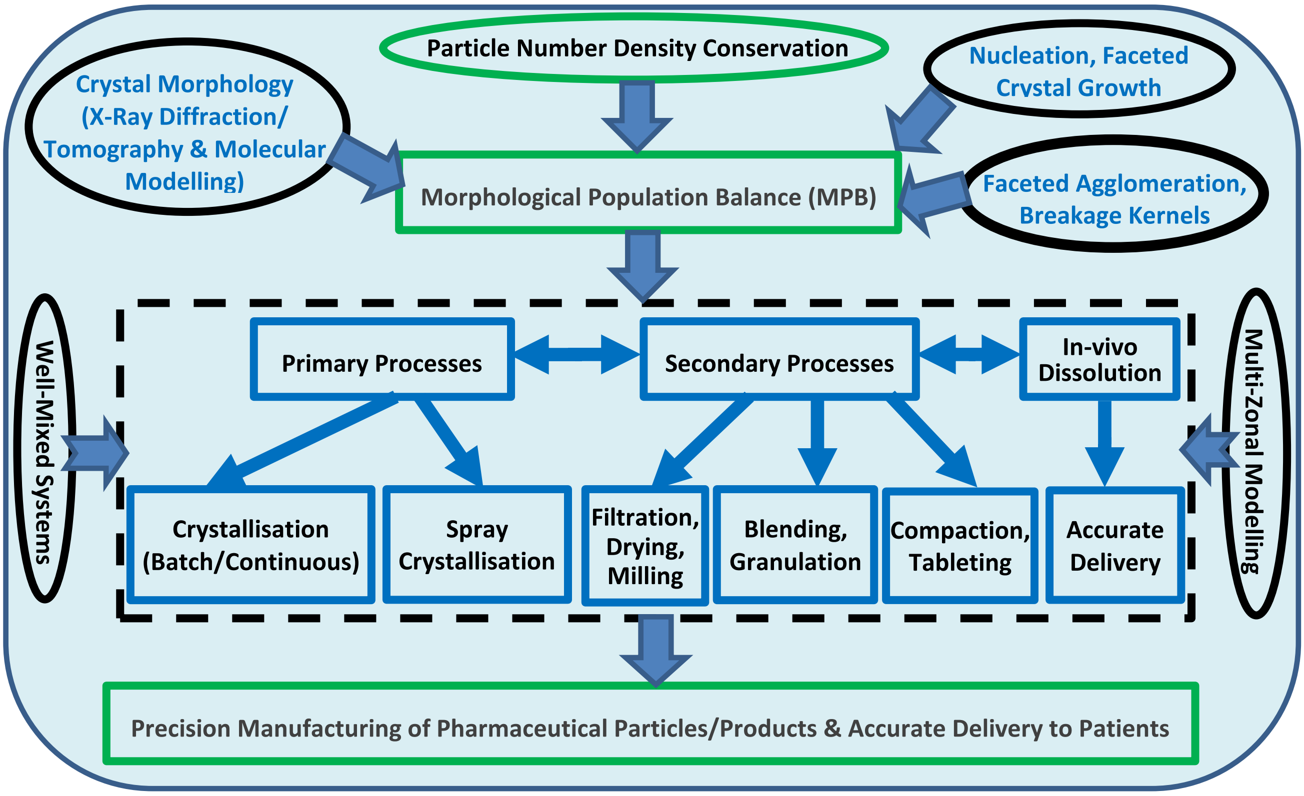

Figure 1. Schematic highlighting the morphological population balance modelling methodology and its wider applicability.

2. APPLICATION OF MORPHOLOGICAL POPULATION BALANCE FOR CRYSTALLISATION PROCESS MODELLING

Crystallisation is a very important unit operation for the separation and purification of many speciality pharmaceutical compounds, hence producing crystals with the facet linking properties in the first stage during the pharmaceutical manufacturing processes. Reflecting their crystallographic structures, many APIs exhibit needle-like or plate-like morphologies and the influence of these crystals on the downstream processes such as washing, drying, filtration, blending, granulation, compaction etc. have attracted much more attention. In order to produce the required crystal properties including shape/size distribution, the first principles-based digital design of crystallisation processes using MPB modelling techniques is attractive (Figure 2). An important feature of MPB models is their ability to predict the full shape distribution of crystals (shape and the corresponding number of crystals), i.e., the shape of each crystal in a crystalliser is predicted during the crystallisation processes. This provides much more powerful manipulation methods to effectively control both the crystal shape and size during and at the end of the crystallisation processes. In this, parameters related to nucleation, crystal growth, agglomeration and breakage, together with solute and solvent properties are needed. These should be measured, predicted or be parameters identified within the MPB models[31].

Classical nucleation theory[32-34] can lead to several empirical or semi-empirical methods to determine nucleus interfacial tension and nucleus size through induction time, supersaturation. Recently, KBHR (Kashchiev, Borissova, Hammond, Roberts) developed an analytical approach[35, 36] to determine key nucleation parameters and also classify nucleation mechanisms by differentiating between instantaneous and progressive nucleation processes. In addition, secondary nucleation in crystallisation processes can affect the final product properties, leading to a broadening of the size and shape distributions. Shiau and Lu[37] studied solute clustering in the diffusion layer around a growing crystal by using PB to simulate the evolution of the cluster size distribution due to the simultaneous aggregation and breakage of solute molecules in the diffusion layer around a growing crystals in a stirred solution. Kitamura and Hayashi[38] studies secondary nucleation behaviour and mechanism in antisolvent crystallisation of thiazole derivative polymorphs. This kind of nucleation kinetics/mechanisms could provide further information of nucleus structure (size/shape), nucleation rate, nuclei distribution, hence linking with MPB modelling.

Generally there are several growth mechanisms (e.g. [4, 39, 40]) including screw dislocation (BCF), birth and spread (B&S) and rough interface (RIG). The face specific growth mechanism is affected by surface chemistry, solid-solution interface, etc., which can link with process operating conditions. Using optical microscopy and an appropriate growth cell, the growth behaviour (rate) of some individual crystal faces can be directly measured[41] under static conditions and as a function of operating conditions and analysed using growth kinetic methods to identify and obtain the corresponding growth mechanisms/kinetics and their parameters. For molecular materials such as pharmaceutical compounds, the growth process can be quite complex with series resistances emulating from both the mass transfer between the bulk solution and the crystals, and from the absorption process at the growth interface. Often the latter can dominate and hence the role of reactor hydrodynamics in facilitating mass transfer is not as significant as one intuitively would expect with the energetics of interfacial surface absorption/step migration process often being the sole rate determining step. Indeed, based on the recent study[42], the measured facet growth rates from single growth-cell experiments were found to comparable with those measured within a real crystalliser.

Agglomeration and breakage in crystallisation processes can be very complicated and overall poorly investigated. Traditionally, agglomeration process in solution is assumed to be controlled by particle collision frequency and agglomeration efficiency, forms the agglomeration kernel by the product of these two terms. Ochsenbein et al.[43] attempted to extend the traditional agglomeration kernel to address the agglomeration of needle-like crystals in suspension by introducing two characteristic sizes, representing a needle-like crystal as a cylinder, into the collision frequency and agglomeration efficiency terms to replace the single characteristic size, the diameter of a sphere. Eisenschmidt et al.[44] estimated the aggregation kernel by the use of Laurent polynomials with in-silico experimental data. For crystal breakage, generally all particles are treated as equivalent spheres with the same volumes, and a spherical mother particle will break into two daughter spheres with equal half volume of the mother sphere for each.

Grof et al.[45] developed a method to investigate needle-shaped crystal breakage by firstly using a DEM of needle-shaped particles to find out the appropriate types of the breakage kernel and the daughter distribution functions, then forming and solving a PB model of breakage with experimental data to determine the material-specific parameters appearing in the breakage functions. There rarely exists any attempt to integrate crystal agglomeration and/or breakage mechanisms on the basis of individual faces with the MPB modelling techniques. For seeding crystallisation processes, the widely used practice for preparing seeds is to mill and/or sieve crystals, hence most of the seeds prepared are broken crystals with the desired size distribution. In literature, again there has been no significant attempt to take into account of the broken crystals as seeds for the simulation of seeded crystallisation processes.

In crystallisation processes, supersaturation, S (= solute concentration / solubility), is the driving force for crystal growth. It determines the facet growth rates based on their inherent interfacial growth mechanisms. As different crystal faces have different growth mechanisms, the facet growth rates as a function of supersaturation can be fast or slow for individual faces, hence resulting in the corresponding faces to grow at various speeds. This leads to crystal shape (and size) evolution during the crystallisation processes, hence potentially achieving process optimisation and control. Cooling (or heating) rate is a very effective tool to change supersaturation, then growth rates, crystal shape. Besides this, seeds conditions (loading, size/shape) and seeding temperature may also be used to optimise and control a crystallisation process to achieve the required properties including crystal shape.

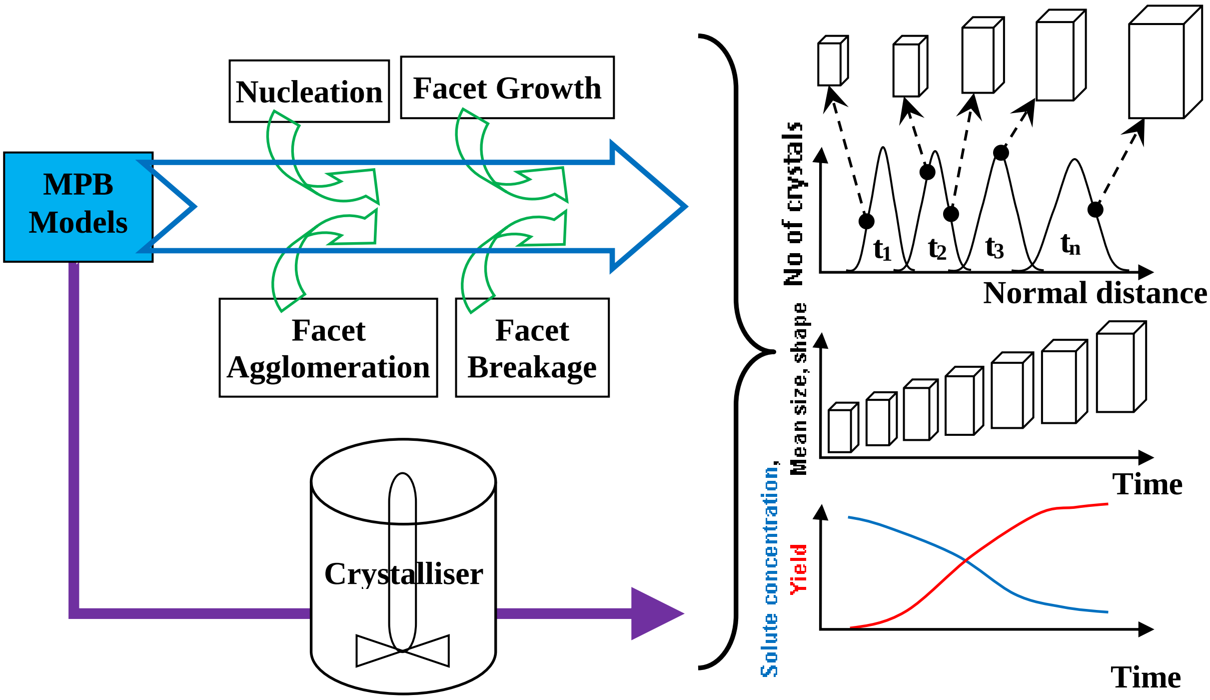

Figure 2. Schematic of MPB for pharmaceutical crystallisation processes and examples of modelling outputs (top right: evolution of crystal size distributions during crystallisation times (t_1, t_2, t_3, …, t_n) with any point on the distribution representing one crystal shape and its corresponding number of crystals having the same shape; middle right: evolution of crystal mean size/shape during crystallisation process; bottom right: solute concentration and crystal yield against crystallisation time).

2.1 Population Balance Modelling

Like the conservation of mass or energy in a system, the PB follows the conservation law on particles (or discrete objects) to describe their evolution during a process. This generally involves both the motion of particles in the system through their defined domains and their birth/death process that can both terminate existing particles and produce new particles. The generic equation of multi-dimensional population balance model governing number density of particles includes the accumulation of particle number density, the convection due to the motion of particles in the spatial space (external coordinates), the convection due to particle growth (or dissolution) in the internal space of particles (such as shape, size, volume, porosity, etc.), particle nucleation, the agglomeration and breakage of particles, and also the net change of particle number density due to the inlet and outlet flows of the system. Therefore PB models are (m + 3) dimensional with 3 representing three external dimensions for the locations of particles in a system and m being the internal variables of particles and particle properties such as porosity, surface energy etc. Further detail on PB modelling can be found in literature [9, 11, 31, 46, 47].

As shown in Figure 3, crystals have shape and size. Strictly speaking, crystal size and its distribution cannot be accurately predicted without accurate prediction of the shape and its distribution. For a population of crystals (dissolving or crystallising) in a crystalliser to manufacture pharmaceutical materials, the evolution of these crystals in terms of both size and shape is not well investigated using PB techniques. Traditionally, PB methods treat faceted crystals as their volume equivalent spheres with volume equivalent diameters (e.g., [1-8, 10]), regardless of their actual shapes (cubic-like, plate-like, or needle-like ...). Therefore the shape information, hence face-specified properties, is lost by the simplification[11]. For needle-like particles such as hydroquinone, potassium dihydrogen phosphate, β-form L-glutamic acid and some pharmaceutical crystals (see for example, [15, 46, 48-54]), researchers usually simplify the shape into two-dimensional system, i.e. length and width, with the width equalling to depth.

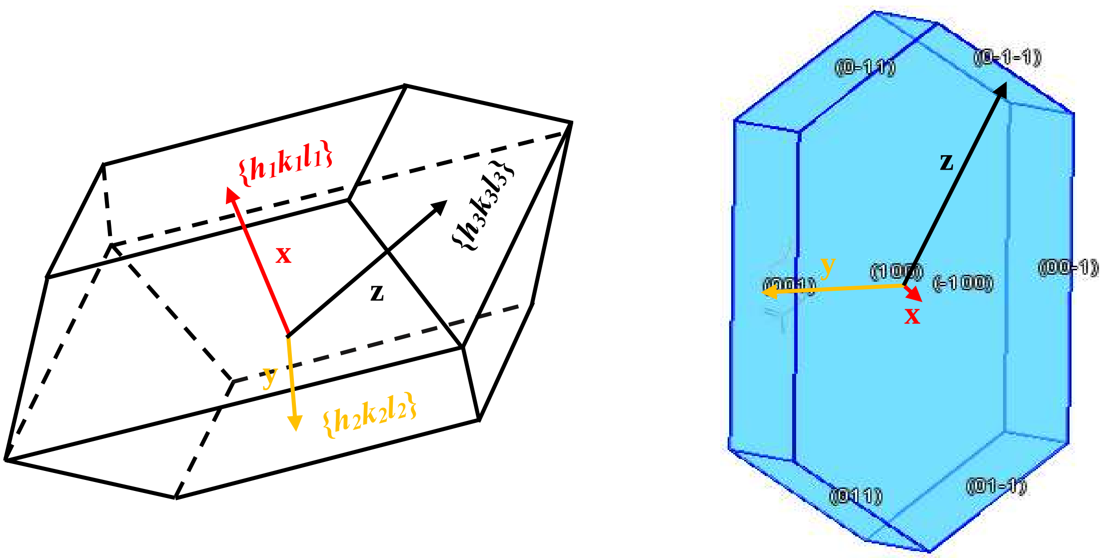

(a) **(b)**

Figure 3. (a) Schematic crystal morphology highlighting the definitions of the three independent dimension variables (x, y, z) for MPB modelling in relation to the crystal morphology defined by e.g. 3 forms ({$h_1k_1l_1$}, ({$h_2k_2l_2$}, ({$h_3k_3l_3$}); (b) The ibuprofen crystal shape and its three variables, x, y and z, representing the normal distances of faces {001}, {100} and {011}, respectively.

2.2 Morphological Population Balance Modelling

The MPB models identify the individual crystal faces with the help of crystal morphology predications, then define the corresponding normal distances from these faces to the centre of the crystal as individual dimensions for forming multi-dimensional, morphological based PB equations[11, 16, 18, 29-31, 55-58]. The solution of these equations simulates the dynamic evolution of these normal distances for a population of crystals during a crystallisation process, and with the known crystal morphology, the dynamic crystal shape and size distributions can be established from these normal distances. Researches were also carried out to extend and generalise the MPB concepts for different cases including the simulation of a population of asymmetric crystals, inclusion of face appearance and disappearance, the influence of crystal growth modifiers, modelling investigation of protein crystallisation processes etc.[12, 55-57, 59-63]. Two-dimensional PB was applied to simulate the crystallisation of potash dihydrogen phosphate (KDP) with high resolution algorithms[15]. The KDP crystals was treated as a rectangular prism i.e. one dimension for length and another dimension for width with width equalling to depth. The real morphology of crystals is still not directly integrated with PB modelling, though the modelling results should be more accurate and representative than one-dimensional (1D), i.e. volume equivalent diameter, with spherical assumption. Ma et al.[11] and Wan et al.[18] focused on the initial methodology development of the MPB which, for the first time, directly integrated the real morphology with PB modelling. However, it was only applied to inorganic materials such as potash alum for demonstration. Singh and Ramkrishna[17] presented a generalised framework for dynamics of single crystal morphology and morphology distributions with an application of MPB to a needle-like crystal system of potassium hydrogen phthalate. Borchert and Sundmacher[14] used a meshing algorithm to develop an efficient numerical solution technique based on the method of characteristics. The projections of three-dimensional (3D) crystals were combined with experimental microscopy images for the generation of a look-up table to reconstruct 3D shape from the images.

In pharmaceutical industry, to ensure product quality, crystallisation processes tend to be designed to operate at lower supersaturation with seeding (as suggested in [64]) to suppress secondary nucleation and agglomeration/breakage, therefore in this context the growth process tends to be the dominant one. For a seeded cooling crystallisation processes in a well-mixed batch crystalliser, the effect of nucleation, agglomeration and breakage may be neglected to simplify the application of the MPB to pharmaceutical crystallisation. Therefore the corresponding PB equation can be written as[9, 11, 31, 46]:

$$\frac{\partial \psi(\boldsymbol{X},t)}{\partial t} + \sum_{i=1}^{N} \frac{\partial}{\partial x_i}\left[\psi(\boldsymbol{X},\ t)\ G_i(\boldsymbol{X},\ t)\right] = 0 \qquad (1)$$

where $\mathbf{X}$ is the internal vector with N components, which can be variables related to crystal size, shape, and other properties, ψ is the number population density function of crystals, G_i is the growth rate, t is the processing time.

In this study, as the N components in **X** are normal distances, one initial condition for Eq. (1) will be the size/shape distribution as a function of the N components at the time of zero: $\Psi(X,t)|_{t=o}$. Similarly, the N boundary conditions will be the size/shape distribution with the starting (0) and finishing (F) values of the N components (i.e. normal distances), i.e. $\Psi(X,t)|_{X=X_0} = \Psi(X_0,t)$ and $\Psi(X,t)|_{X=X_F} = \Psi(X_F,t)$. For batch crystallisation processes, there is no crystal passing through the boundaries, hence, $\Psi(X,t)|_{X=X_0} = 0$ and $\Psi(X,t)|_{X=X_F} = 0$.

For MPB models, the internal variable should include the variables which can accurately represent (and re-construct) particles shape, such as the normal distances of individual faces of crystals (Figure 3). By applying the MPB methodology, the normal distances from faces $\{h_1k_1l_1\}$, $\{h_2k_2l_2\}$ and $\{h_3k_3l_3\}$ to the crystal centre can be defined as three independent dimension variables (x, y, z), respectively, as shown in Figure 3a. It is worth to note that three dimensions (x, y, z) are not Cartesian coordinates, hence they are not perpendicular to each other. The developed MPB equation for seeded cooling crystallisation process in a well-mixed batch crystalliser with negligible agglomeration, breakage and nucleation can be re-written from Eq. (1) as:

$$\frac{1}{V_T(t)}\frac{\partial}{\partial t}[\psi(x,y,z,t)\,V_T(t)] + \frac{\partial}{\partial x}[G_x(x,t)\,\psi(x,y,z,t)] + \frac{\partial}{\partial y}\left[G_y(y,t)\,\psi(x,y,z,t)\right] + \frac{\partial}{\partial z}[G_z(z,t)\,\psi(x,y,z,t)] = 0 \quad (2)$$

where V_T is the total volume; x, y, z three independent dimension variables; G_x, G_y, G_z growth rates in x, y, z directions. The corresponding boundary conditions for Eq. (2) will be $\Psi(x,y,z,t)|_{x=x_i} = 0$, $\Psi(x,y,z,t)|_{y=y_i} = 0$, $\Psi(x,y,z,t)|_{z=z_i} = 0$ (i = 0 or F) with the one initial condition being$\Psi(x,y,z,t)|_{t=o}$. Note that the assumption of negligible agglomeration, breakage and nucleation is generally applicable only under some typical conditions such as low superstation, low agitation rate, and seeded processes.

3. MATERIALS AND COMPUTATIONAL MEHTODS

3.1 Crystal Morphology, face-specific growth rates and growth mechanisms

In this study, solute-solvent system of pharmaceutical compound, ibuprofen, crystallised from ethanol was used. Ibuprofen can be crystallised from a mixture solvents of 95%ethanol and 5%water (case study 1) and water-free ethanol (case study 2) in seeded batch crystallisers. The obtained crystal as the one shown in Figure 3b has 2 {100}, 2 {001} and 4 {011} faces with a monoclinic crystal structure in a $P2_1/c$ space group[41]. Further detail of the system can be found in literature[41, 64-66].

During crystallisation processes, facet crystal growth rate is generally a two-step kinetic process encompassing a balance between the incorporation of growth units onto the crystal surface and the diffusion by mass transfer of the growth units within the bulk of the solution[67]. The growth kinetics can be classified as a number of well-known models including power law[4], birth & spread (B&S) and Burton-Cabrera-Frank (BCF) models[39]. Therefore, the kinetics of a defined crystal growth interface as a function of supersaturation can be modelled as follows[67]:

$$G_{power} = \frac{S - S_{crit}}{\frac{\rho_S}{k_{MT}\, C^* MW_S} + \frac{1}{k_G (S - S_{crit})^{r-1}}} \tag{3}$$

$$G_{B\&S} = \frac{S - S_{crit}}{\frac{\rho_S}{k_{MT}\, C^* MW_S} + \frac{1}{k_G (S - S_{crit})^{-1/6} exp\left(A_1/(S - S_{crit})\right)}} \tag{4}$$

$$G_{BCF} = \frac{S - S_{crit}}{\frac{\rho_S}{k_{MT}\, C^* MW_S} + \frac{1}{k_G (S - S_{crit}) tanh\left(A_2/(S - S_{crit})\right)}} \tag{5}$$

where S is supersaturation defined by the ratio between the solute concentration at a solution temperature and the solubility at the same temperature, S_{crit} is a critical value of supersaturation, k_G is the growth rate constant, r is the growth exponent, A_1 and A_2 are the thermodynamic parameters, ρ_s is the solute density, k_{MT} is the coefficient of mass transfer within the bulk of the solution, MW_s is the solute molecular weight, C* is the equilibrium concentration (solubility). The term $\frac{k_{MT}\, C^* MW_S}{\rho_S}$ $(= k'_{MT})$ in Eqs. (3 – 5) can be treated as a fitting parameter. In Eq. (3), if r = 1, it corresponds to a rough interface growth (RIG) mechanism[40].

In this work, the facet growth rates of the {001 and {011} habit planes of ibuprofen crystals growing in 95%ethanol/5%water were measured in a 0.5 ml UV cuvette cell with optical microscopy[41, 66]. The growth rates in the face directions of {011} and {001} as a function of supersaturation are given in[67]. These data were used to characterise the growth mechanisms as incorporated with the MPB framework.

3.2 Computational Details

The solubility of ibuprofen in a solvent (95%ethanol / 5%water) and the faceted growth rates in the x, y and z face directions of ibuprofen crystals growing from the solvent were obtained from literature[41]. The solubility equation is as follows:

$$C^* = e^{\left(\frac{-3727}{T} + 11.036\right)} \tag{6}$$

where C* is the solubility (kg/kg solvent), T is the solution temperature (^{o}C).

With the obtained solubility and faceted growth rates, the developed three dimensional MPB model was then solved with the following operating conditions for case study 1: cooling rate (CR) of 0.5^{o}C/min, saturation concentration of 1.601 kg/kg (saturated temperature of 35^{o}C), seeding point of 20^{o}C with the corresponding supersaturation, S, of 1.85, seeds loading of 0.5%, and seeds mean x, y and z of 22.9, 25.7 and 44.6 μm.

There is an enormous shortage of experimental data for practical crystallisation processes in general and more pertinently, with regard to this study, relating to the 3D (3 normal distances) morphological related growth rates and crystal size/shape and their distributions. Hence, in case study 2, we have simply validated the 3D MPB simulation results against 1D (volume equivalent diameter) published data. In this, the simulated 3D data were back modelled into its 1D (volume equivalent diameter) form simply to compare and the outcome highlights good agreement.

In case study 2, ibuprofen crystals were grown from water-free ethanol in a 1 L crystalliser[64]. The solubility used is from literature[64, 65] as follows:

$$C^* = 0.497 + 1.026 \times 10^{-3} \times (T - 273.15)^2 \tag{7}$$

At each crystallisation time, a set of 3D mean distances (x, y, z) can be generated by systematically searching through the domains of mean distances (x, y, z), with the ratio of attachment energies of the three crystal faces[66] as a constraint to mean distances (x, y, z). Each set of mean distances (x, y, z) then is converted into 1D sphere-based mean size, volume equivalent diameter (d_{eq}). The d_{eq} obtained from the conversion is compared against the measured d_{eq} [64] to produce the best fitting mean distances (x, y, z) at that crystallisation time. Then the crystal growth rates of ibuprofen in the {100}, {001} and {011} faces can be obtained with the supersaturation and the fitted 3D mean size values as a function of time.

The seeds distributions in the three faces (normal distances x, y and z) were fitted by assuming that their distributions have a Gaussian form with 6 variables, i.e. 3 mean values and 3 standard deviations. With systematic search of these 6 parameters, the 3D size/shape distribution of each search was converted into 1D distribution based on volume equivalent diameter. Then the obtained 1D distribution was compared with the experimentally obtained volume equivalent size distribution[64] and the ratios among the 3 normal distances based on their attachment energies. The 3D size/shape distribution with the least difference is the best fitted one and subsequently used for MPB simulations, in this study, as seeds size/shape distribution (initial condition). The obtained seeds facet distributions in x, y and z directions for MPB modelling were listed as 7.6, 15.2 and 15.2 μm for mean x, y and z and 6, 19 and 60 μm for their corresponding standard deviations. The ibuprofen crystals were crystallised from water-free ethanol in a 1L batch crystalliser with seeding. The process started at a supersaturation of 1.07 with 0.75L solution and a fixed solution temperature of 25°C, and 1.4 g seeds. The detail operating conditions can be found in[64].

For transformation from simulated 3D size/shape distribution to 1D size distribution, the actual volume of each set of x_i, y_j, z_k (i = 1, N_i, j =1, N_j, k = 1, N_k) can be calculated based on the morphology, then the corresponding volume equivalent diameter. With the known number of crystals for the set of x_i, y_j, z_k, the 1D size distribution can be obtained for comparison with the measured one.

PB equations, in particular when including the processes of nucleation, growth, agglomeration and breakage, can be very complicated partial-integral differential equations, which present practical challenges to solve these equations[68]. Actually, it can only be possible to solve them analytically for a few very simple cases. Therefore, a number of various numerical algorithms has been developed in last few decades, including the method of moments, method of characteristics, Monte Carlo techniques, discretisation methods, cell average methods, hierarchical solution strategy, method of classes, finite difference/volume methods etc. (see for example[31, 47, 69] for more detail). In this study, the discretisation method, moment of classes (e.g. [11, 31, 49, 51]), was used to discretise the formed partial differential MPB equation (Eq. (2)) into ordinal differential equations (ODEs). The computational domain of normal distances (x, y, z) was discretised into (n_1, n_2, n_3) classes, in the current case, (70, 70, 70) classes over the size ranges of three normal distances of (100, 120, 160 μm), hence generating 70×70×70 ODEs for numerical solution. With the help of a Gaussian-type shape/size distribution for seeds crystals and other operating conditions, the discretised MPB equations were solved using the Runge-Kutta-Fehlbergh $4^{th}/5^{th}$-order solver[70] with automatic time-step control to obtain the evolution of normal distances in three face directions. Further details can be found in literature (e.g. [11, 16, 31, 49, 51, 52, 70]). The typical seeds distributions for ibuprofen cooling crystallisation in this work are shown in Figure 4.

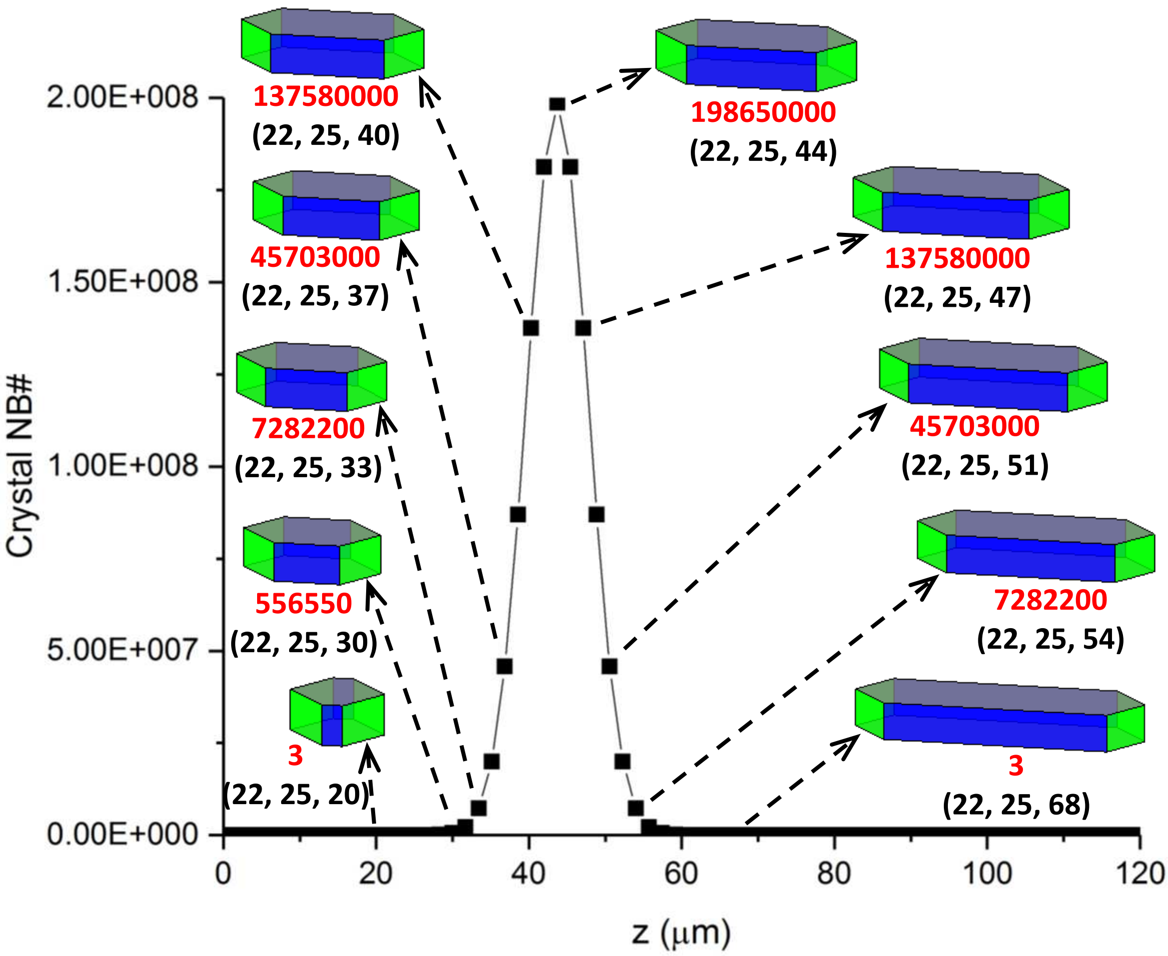

Figure 4. Typical seeds size/shape distributions for ibuprofen crystallisation at the mean normal distances of faces {100} and {001}, i.e. x and y. The grey, blue and green coloured faces of ibuprofen crystals are {100}, {001} and {011} faces, respectively. The red coloured numbers are number of crystals and the values in the brackets represent the normal distances of faces {100}, {001} and {011}.

4. RESULTS AND DISCUSSION

4.1 Case Study 1: Ibuprofen Crystallised from 95%Ethanol/5%Water

By applying the method from[67] and using Eqs. (3 – 5), the growth rate in the face direction of {011} as a function of supersaturation was found to have the best fit of BCF mechanism with the experimental data[41]. The corresponding facet growth rate, G_z (µm/min), is as follows:

$$G_z = \frac{S-1.53}{3.85\times10^{-2}+\frac{1}{4.17\times10^{3}\times(S-1.53)\times tanh\left(\frac{26.99}{S-1.53}\right)}} \tag{8}$$

The fitting of the {001} face growth rate, G_y (µm/min), as a function of supersaturation, also corresponds to a BCF growth mechanism with the following equation:

$$G_y = \frac{S-1.33}{3.85\times10^{-2}+\frac{1}{1.7\times10^{2}\times(S-1.33)\times tanh\left(\frac{50}{S-1.33}\right)}} \tag{9}$$

Although the crystal growth mechanisms for both faces {011} and {001} are BCF, it was found that the term related to mass transfer has a value of 3.85×10^{-2} which is about one magnitude higher than that of the surface integration term (see Eq. (8)), hence the growth of face {011} is a diffusion limited process, whilst both terms have very similar values as shown in Eq. (9), which means that the growth of face {001} is controlled by both diffusion (mass transfer) and surface molecule integration processes.

As the growth in the {100} direction of ibuprofen crystals was found to be very slow, the growth rate in the {100} face direction, G_x (μm/min), was estimated as a proportion (10%)[71] of G_y.

The predicted solution temperature, supersaturation, crystal concentration, mean normal distances $(\bar{x}, \bar{y}, \bar{z})$ for faces {100}, {001}, {011}, and the corresponding faceted growth rates with a cooling rate of 0.5°C/min are plotted in Figure 5. Under this cooling rate, the supersaturation of ibuprofen solution increased with time when solution temperature was reduced (Figure 5a). During the cooling crystallisation process, the change of supersaturation is the result of competition between the decrease of solute concentration caused by the consumption of solute due to solute molecules growing onto crystal surfaces and the reduction of solubility due to the decrease of solution temperature. In the current case, the solubility decrease of ibuprofen in the mixture of 95%ethanol/5%water is faster than the decrease of ibuprofen concentration due to slow solute consumption by crystal growth. Therefore, the supersaturation was found to increase, which lead to the increase of faceted growth rates (Figure 5c) with time. Figure 5b showed that the mean normal distance for face {011} increased rapidly with time, while less growth happened in x direction as the face {011} is the fastest growing face from previous studies [41, 71].

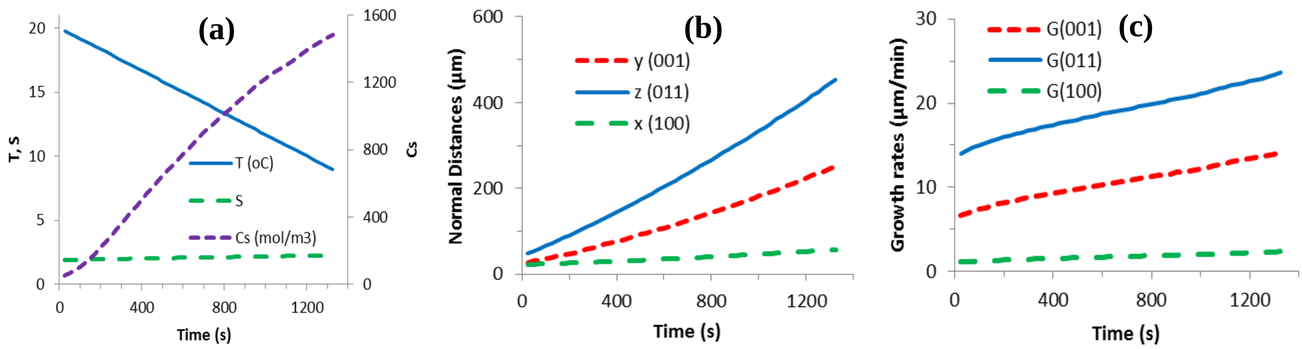

Figure 5. Simulation results of ibuprofen crystallised from %95ethanol/5%water (case study 1) using MPB with CR = 0.5°C/min: (a) solution temperature (T), supersaturation (S), crystal concentration

(Cs), (b) evolution of mean normal distances (x, y, z), and (c) facet growth rates in x, y, z face directions.

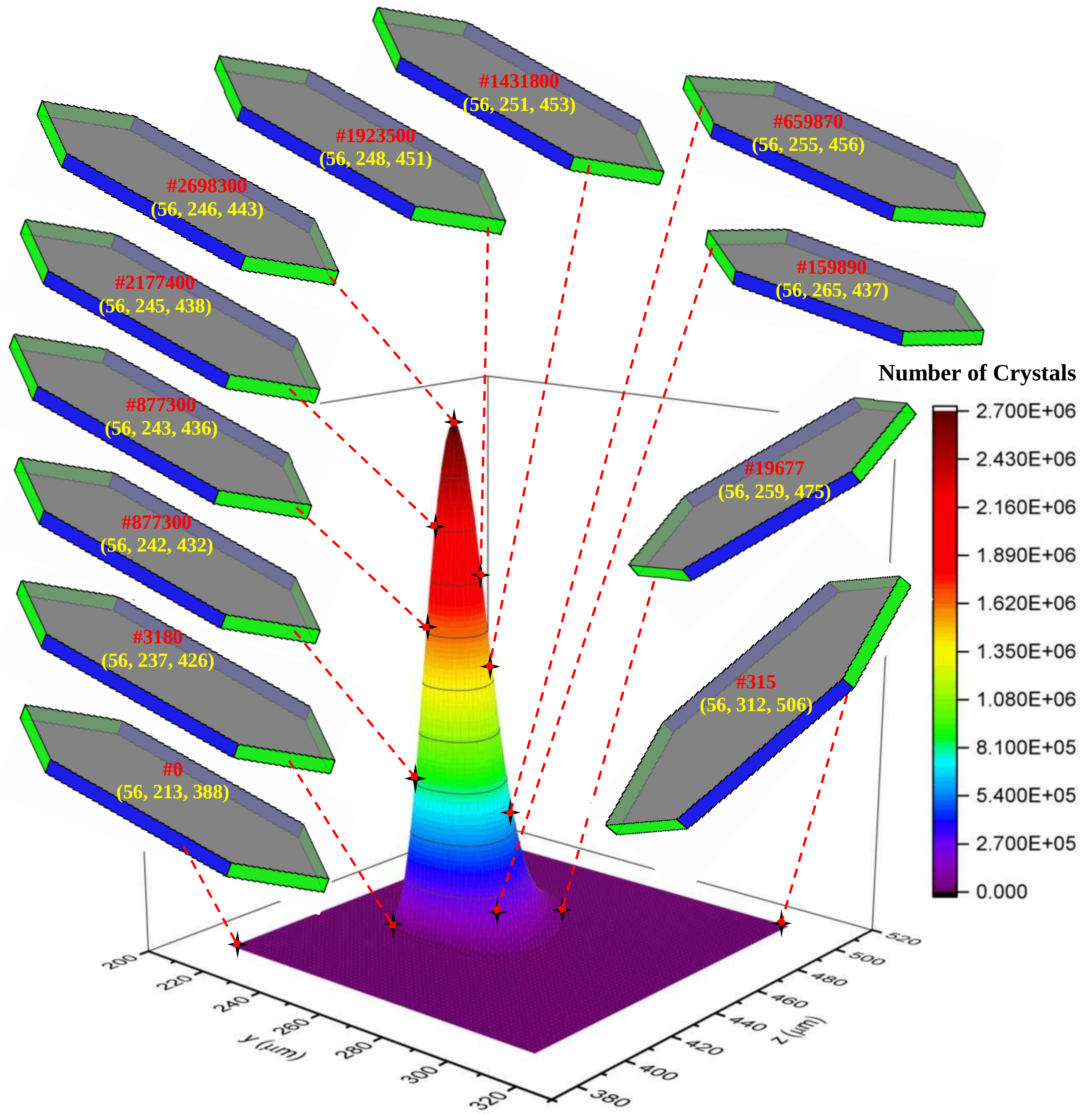

Figure 6. Typical size/shape distribution of ibuprofen crystals at a fixed normal distance, x, of 56 μm with other two normal distances (y, z) varying from (213 μm, 388 μm) to (312 μm, 506 μm), and also random points of normal distances (x, y, z) with their corresponding crystal shapes. The grey, blue and green coloured faces of ibuprofen crystals are {100}, {001} and {011} faces, respectively. The red coloured numbers are number of crystals and the values in the brackets represent the normal distances of faces {100}, {001} and {011}.

Some crystal mean shapes at different processing times are plotted in Figure 6. Overall, face {011} grew faster than face {001} as shown in Figure 7. The increase speed of both growth rates against crystallisation time is very similar (Figure 5c). As both faces have grown much faster than face {100}, the ibuprofen crystals were observed to become more and more plate-like (Figure 7). To be consistent with current practice, Z is the mean in long axis, which can be calculated based on mean normal distance in z direction and the crystal morphology of ibuprofen. Y and X are as same as mean normal distances in y and x directions in this case. The mean aspect ratio of Z/X and Y/X was found to increase slightly from 2.4 (seeds) to 2.7, then reduce very slowly to 2.6. Note that the use of aspect ratio to demonstrate crystal shape evolution is only one of the results visualisation methods as aspect ratio is widely used in academic and industrial communities. However, for accurate and comprehensive presentation of face-based modelling and measurement data, other methods for visualising and disseminating shape information should be explored and developed for the wide application of MPB.

The mean surface area evolution of different faces and the percentages of contribution during the ibuprofen crystallisation process are plotted in Figure 8, with the spherical area, converted from MPB results based on the volume equivalent assumption, being in dotted black line. The areas of both faces {011} and {001} increased very slowly, while face {100} enlarged dramatically (Figure 8a). This demonstrates that face {100} dominates the surface evolution of ibuprofen crystals due to its slowest growth, which contributes 44 ~ 75% (0 ~ 1300 s of crystallisation time) of the total surface area, but faces {011} and {001} only accounts for 27 ~ 12% and 29 ~ 13%, respectively (Figure 8b). Comparing with the evolution of the actual surface area (black line in Figure 8b) based on MPB modelling, the spherical surface area can only reach 78 ~ 84% which is smaller than the real total surface area of the three faces.

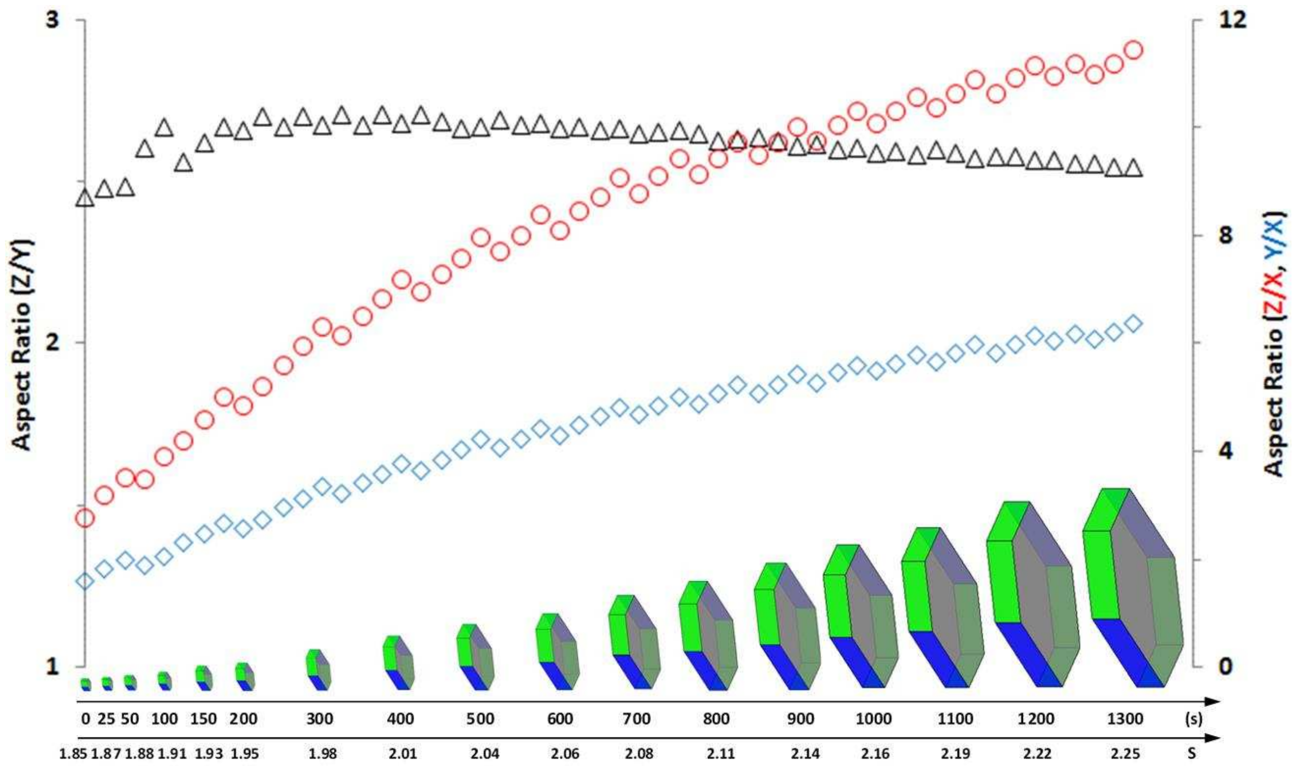

Figure 7. Simulated mean shape evolution of ibuprofen crystallised from a mixture of 95%ethanol/5%water (case study 1) with CR = 0.5ºC/min (Aspect ratios: △ - Z/Y; ○ - Z/X; ◇- Y/X). The grey, blue and green coloured faces are {100}, {001} and {011} ibuprofen faces, respectively.

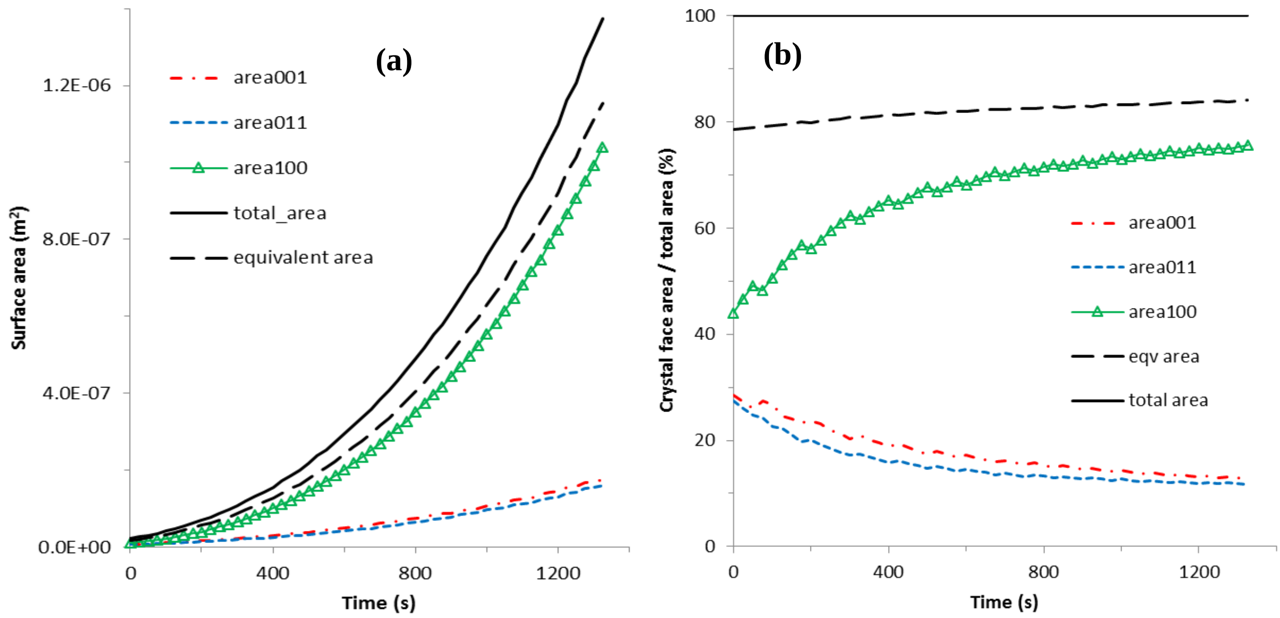

Figure 8. (a) Mean surface area evolution of different faces and (b) the area percentage of individual faces and total surface area during crystallisation of ibuprofen crystals from a mixture of 95%ethanol/5%water (case study 1) with CR = 0.5ºC/min as predicted with the MPB technique.

4.2 Case Study 2: Ibuprofen Crystallised from Water-Free Ethanol

The obtained facet growth rates of three faces {011}, {001} and {100} via fitting the volume equivalent growth (converted from the facet growth) with the measured growth[64] are as follows:

$$G_z = 7.9005 \times (S - 1) \quad (10)$$

$$G_y = 7.0226 \times (S - 1) \quad (11)$$

$$G_x = 1.1704 \times (S - 1) \quad (12)$$

and also shown in Figure 9. The {100} face growth rate is around 6 ~ 7 times lower than the {001} face, which is similar to the estimation in literature[71].

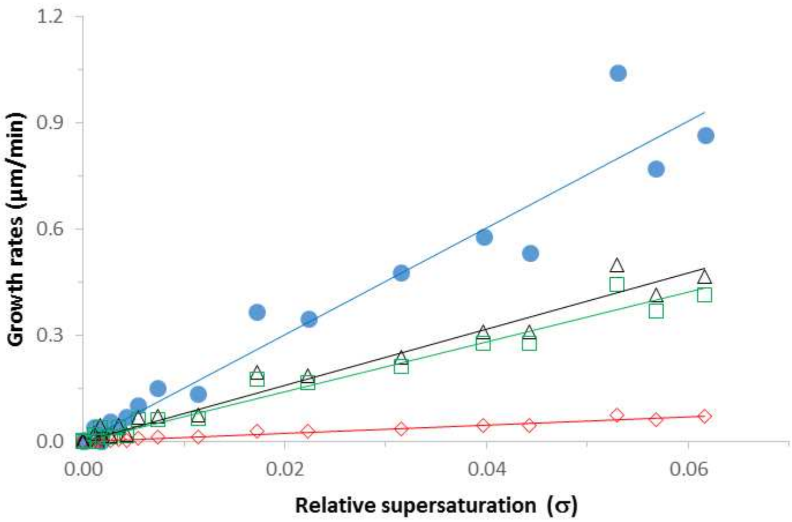

Figure 9. Growth rates vs. relative supersaturation (σ = S-1). Blue solid dots – growth rate based on equivalent diameter from experimental data[64]; Open symbols – face-based fittings to the experimental data for {011} face (black), {001} face (green) and {100} face (red); Lines – fitting results for growth rate based on equivalent diameter (blue), {011} face (black), {001} face (green) and {100} face (red). Note that the experimental data points for the growth rate based on equivalent diameter were calculated using the corresponding data points of equivalent diameter, as a function of time, as extracted from the paper by Rashid et al.[64]. The corresponding data points of supersaturation as a function of time were also extracted from[64]. Combining the calculated experimental growth rate and extracted supersaturation provided the dataset for the experimental growth rates based on equivalent diameter (Blue solid dots) and the associated fitted regression line (Blue line).

The evolution of normal distances simulated using MPB and the corresponding volume equivalent spherical diameter converted from the simulated normal distances are plotted in Figure 10, together with the face-based growth rates and the corresponding one-dimensional growth rate based on volume equivalent spherical diameter. The spherical-based diameter and growth rate obtained directly from experimental measurements[64] are also plotted in Figure 10 for comparison. It can be seen that the face {100} grew much slower than other two faces {011} and {001} as expected. The evolution of diameter and growth rates based on volume equivalent spheres are in generally good agreement with the experimental data[64]. The MPB results show that the crystals in the crystalliser barely had any growth after 400 min, while the experiment produced the similar trend after 400min but with some growth towards the end of the process at 1200 min.

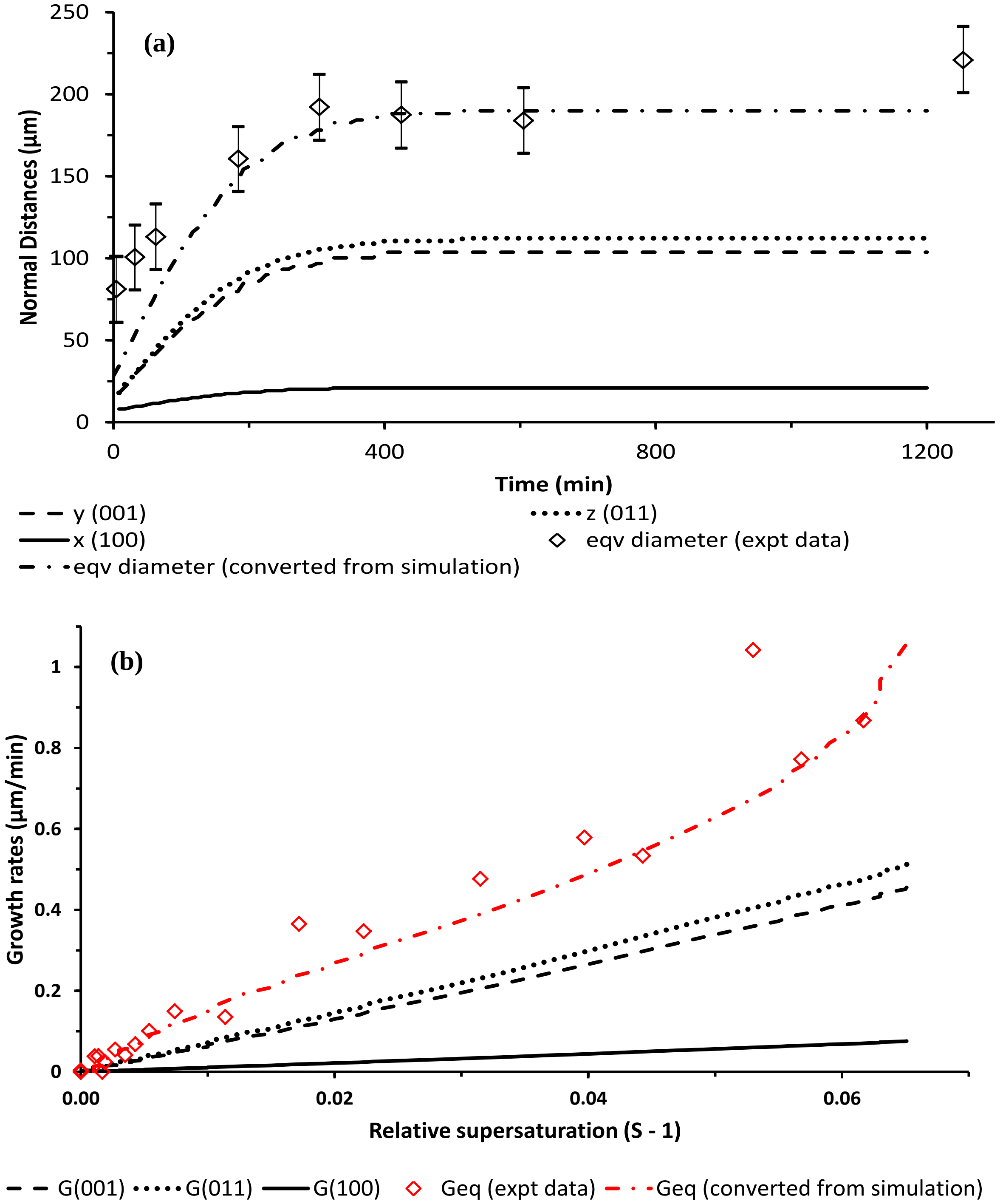

Figure 10. Simulation and measurement results of ibuprofen crystallised from ethanol (case study 2) using MPB. (a) evolution of mean normal distances (x, y, z) and volume equivalent diameter (d_{eq}); (b) facet growth rates (G_x, G_y, G_z) in x, y, z face directions and growth rate based on volume equivalent diameter (G_{eq}): Solid, dash, dot lines – (x, y, z) or (G_x, G_y, G_z); Dash and dot line – d_{eq} or G_{eq} converted from the simulated normal distances, diamonds - d_{eq} or G_{eq} measured by experiment.

Figure 11 shows the predicted supersaturation and crystal volume equivalent diameter with the corresponding experimental data from[64]. Overall the simulated supersaturation and equivalent diameter generally well reproduced the experimental data. The slower growth of volume equivalent diameter led to the slower consumption of solute (as the experiment was performed at a constant solution temperature of 25°C), hence the slower decrease of supersaturation. Note that the input data such as initial size distribution and growth rates in three face directions for the MPB simulation were estimated from volume equivalent ones, not direct measurements. Therefore their values may not be accurate for MPB modelling and validation.

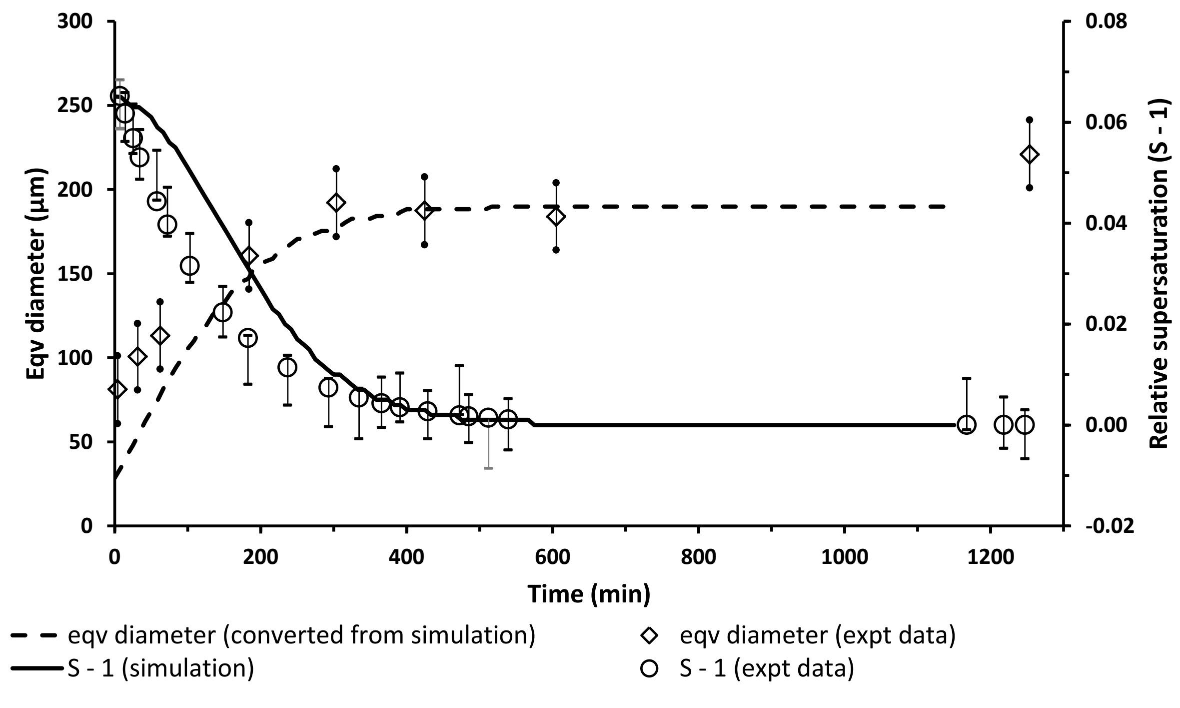

Figure 11. Simulated and measured relative supersaturation and crystal volume equivalent spherical diameter during crystallisation process of ibuprofen (case study 2). (Solid line – predicted supersaturation; Dash line – predicted equivalent diameter; Circles – measured supersaturation with error bars; Triangles – measured equivalent diameter with error bars.

The mean shape evolution of ibuprofen crystallised from pure ethanol at a constant solution temperature of 25°C is plotted in Figure 12, with the aspect ratios between three directions. It can be seen that the crystals grew bigger at the first 400 min, then the growth became much slower. This corresponds to the variation of supersaturation during the process as shown in Figure 11. The shape of ibuprofen crystals becomes more flat, i.e. the aspect ratios between faces {011} and {100} increased from 1.4 at 1 min (seeds) to 3.6 at 400 min and then 3.8 at 1100 min, even at such a low supersaturation range (S < 1.1) of the whole process. At higher operating supersaturation, the shape evolution and aspect ratio can be expected to be more significant.

Figure 13 shows the MPB predicted surface area evolution of individual faces and corresponding contributions of individual faces to total crystal area when crystallising ibuprofen from pure ethanol with a fixed temperature of 25°C. The spherical area and its contribution, based on volume equivalent assumption and converted from MPB modelling results, are also plotted in Figure 13. The area of face {100} increases rapidly, reaching over 70% of the total crystal area, while other two faces, {011} and {001}, had a slower increase of surface areas with < 20% and < 10% contributions to the total area. The spherical based surface area (black dash line in Figure 13) has a contribution of 82 - 92%. However, the predicted surface areas of individual faces, together with their surface properties, will provide accurate digital design of the crystallisation process and also downstream processes.

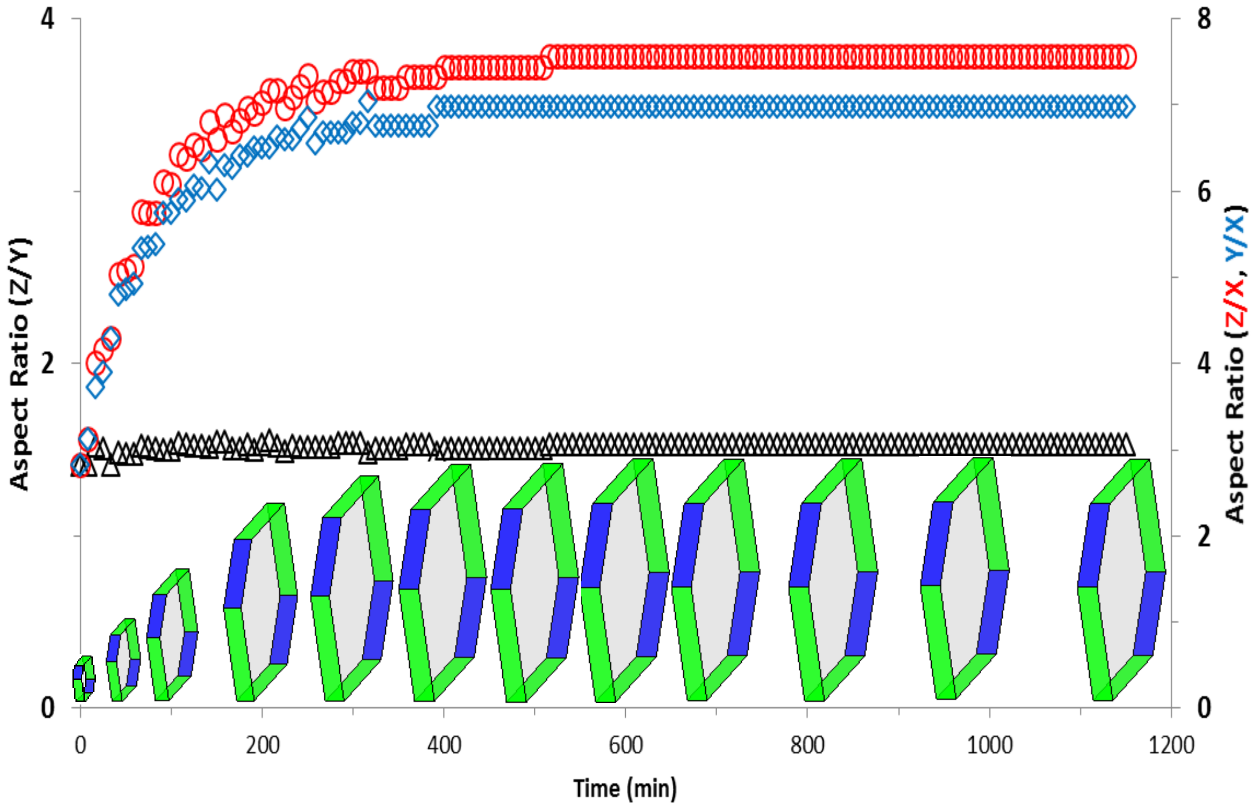

Figure 12. Mean shape evolution of ibuprofen crystallised from pure ethanol (case study 2) with a constant solution temperature of 25°C (Aspect ratios: △ - Z/Y; ○ - Z/X; ◇- Y/X). The grey, blue and green coloured faces are {100}, {001} and {011} ibuprofen faces, respectively.

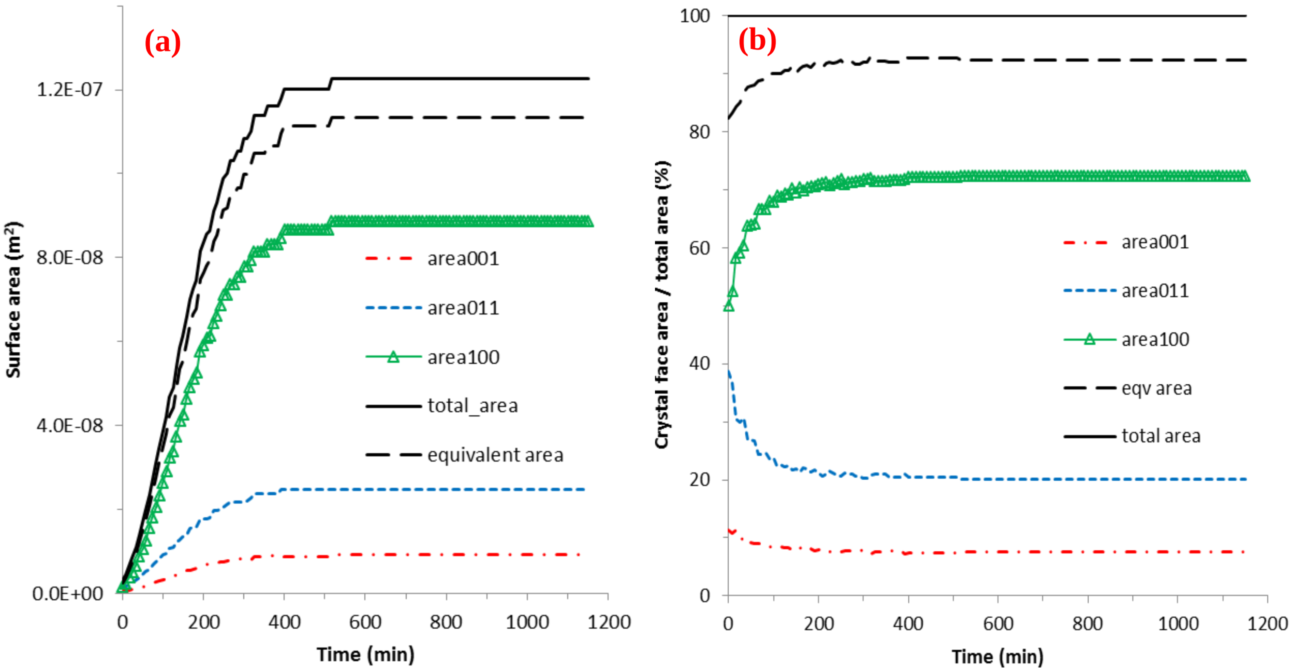

Figure 13. MPB predicted (a) surface area evolution of different faces and (b) area percentage of individual faces and total surface area when crystallising ibuprofen crystals from pure ethanol (case study 2) with a fixed temperature of 25°C.

Figure 14 shows the evolution of crystal size distribution (CSD) at six crystallisation times (30, 60, 180, 300, 420 and 1200 min). As the face {100} grew very slow, the mean values of the face {100} normal distance were fixed at 9.9, 11.6, 17.6, 20.1, 20.9 and 21 μm in Figure 14. The left (coloured as red) projections in Figure 14(a-f) represent the size distributions of face {011} with the normal distances of faces {100} and {001}, (x, y), being fixed at their mean values of (9.9, 30 μm), (11.6, 40.3 μm), (17.6, 79.7 μm), (20.1, 96.9 μm), (21, 103.7 μm) and (21, 103.7 μm) for the six crystallisation times. Similarly, The right (coloured as blue) projections in Figure 14(a-f) show the size distributions of face {001} at the six crystallisation times with the mean (x, z) values of (9.9, 30 μm), (11.6, 43 μm), (17.6, 84.9 μm), (20.1, 105.4 μm), (21, 110.6 μm) and (21, 112.3 μm). Based on the ibuprofen morphology as shown in Figure 3b, each set of normal distances (x, y, z) at a crystallisation time can be used to reconstruct the shape of the ibuprofen crystals. Together with the corresponding number of crystals and their associated normal distances as a function of time, the ibuprofen shape distributions can be obtained for any crystallisation time. This capability provides important information for precision product design not only regarding crystallisation processes but also those related to downstream processes where particle shape and surface chemistry plays a role, e.g. filtration, drying, blending, compaction etc.

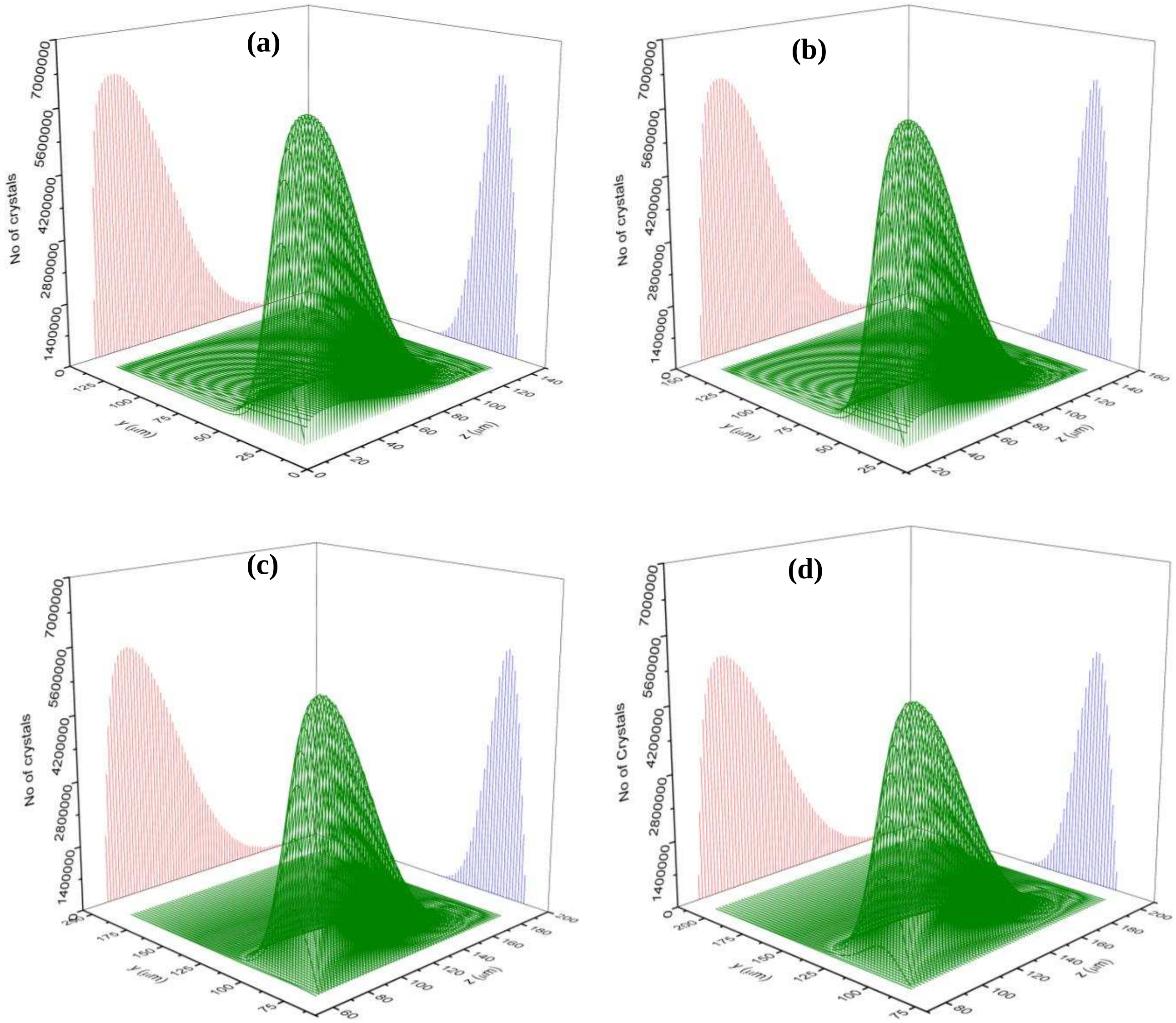

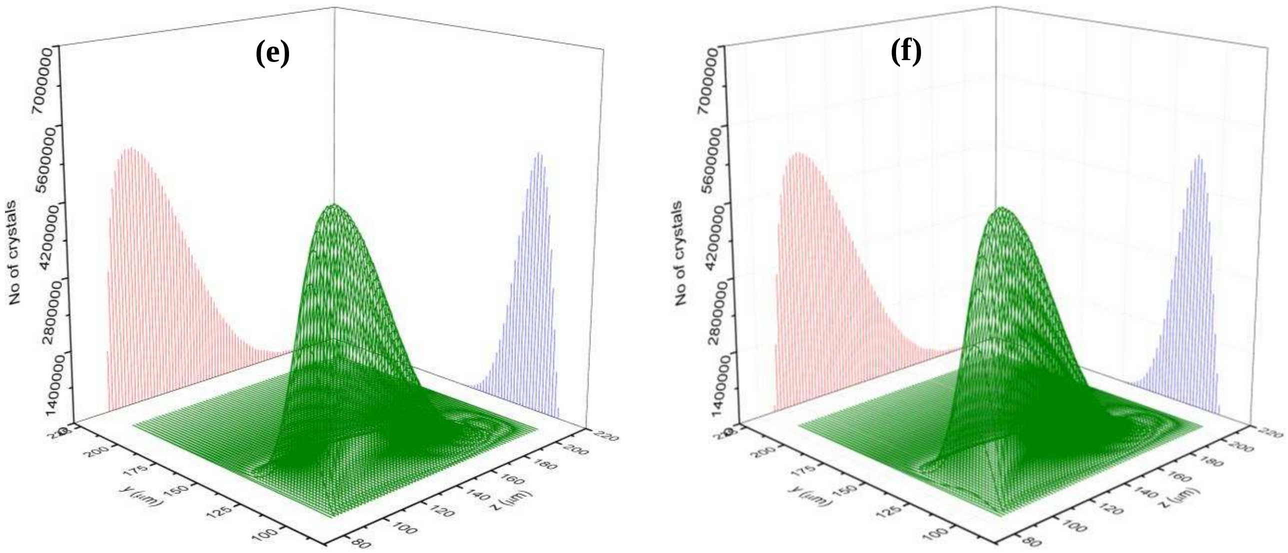

Figure 14. Evolution of some typical crystal size distributions (green) in (y, z) plane with x being fixed at its mean values from MPB simulation results at various crystallisation times (case study 2): (a) 30 min, (b) 60 min, (c) 180 min, (d) 300 min, (e) 420 min and (f) 1200 min. The left (red) and right (blue) projections are the size distributions of face {011} at mean (x, y) values and face {001} at mean (x, z) values, respectively.

To compare the CSD from MPB modelling with experimental data[64], the simulated CSD values using MPB were converted to one-dimensional CSD based on volume equivalent spherical diameters, which are plotted in Figure 15, together with the experimental determined CSD. At the early stages (< 180 min), the agreement between the measured CSDs and converted ones from MPB modelling results is considerably good. However, the standard deviations of converted CSDs become much smaller than the measured CSDs at the later stages, though their mean sizes are very similar at different crystallisation times. As mentioned before, the input data for the MPB simulation in this case study, including initial face-based CSD and facet growth rates were estimated from volume equivalent experimental data, which, together with the volume equivalent experimental data (as the crystals are needle-like), can most possibly contribute to these discrepancies. Therefore the accurate measurements of crystallisation kinetics and crystal properties (facet growth, size/shape and distributions etc.), and also the process data collection and analysis are equally important for MPB model development/validation, and its optimisation/control of crystallisation processes. Further studies in these areas are underway with the advancements to be reported later.

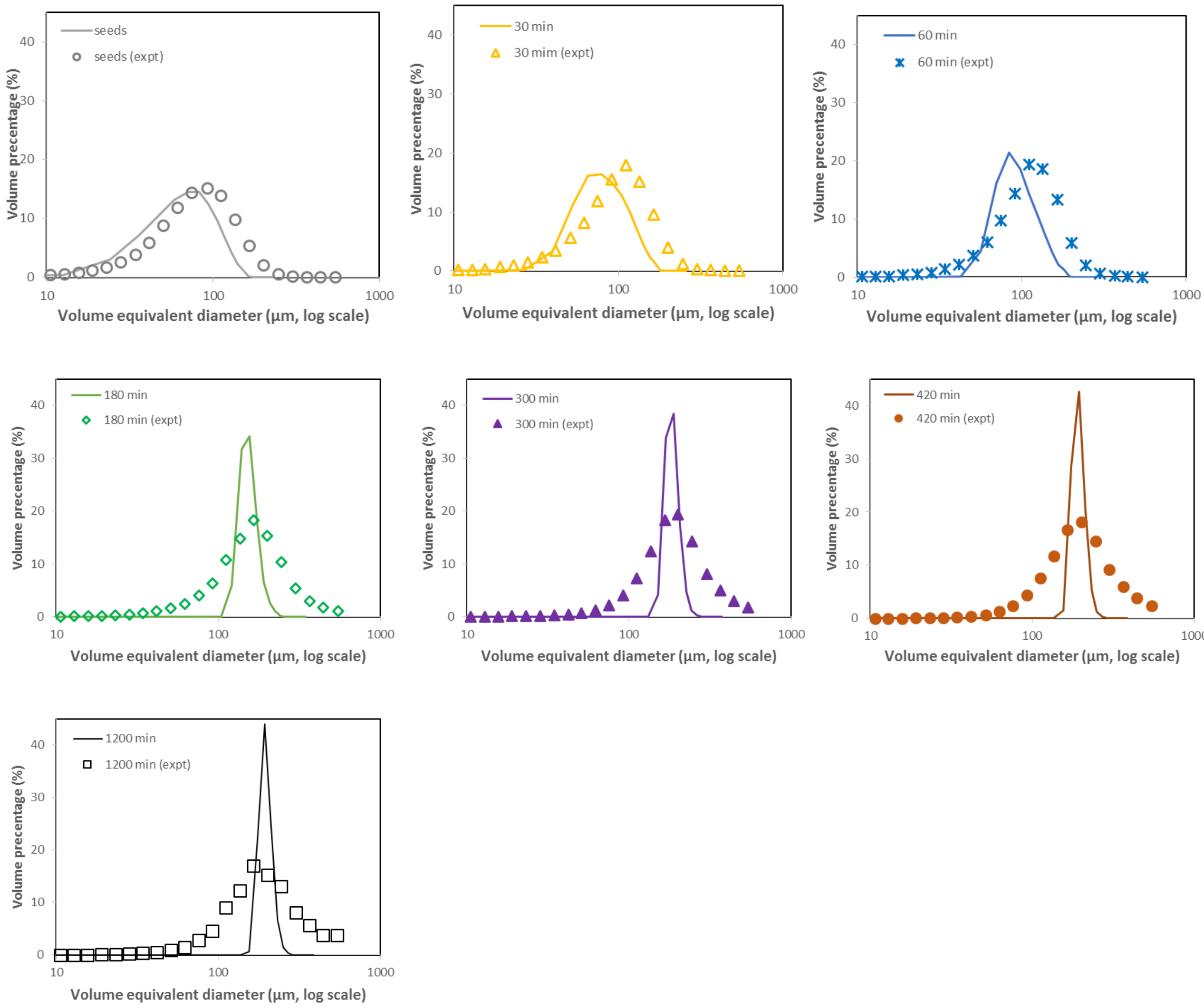

Figure 15. Comparison between the experimentally measured CSD (symbols) and converted CSD (solid line) based on volume equivalent spherical diameters using MPB simulated results at various crystallisation times of 0 (seeding), 30, 60, 180, 300, 420 and 1200 min (case study 2).

5. CONCLUSIONS

The application of the MPB modelling methodology for using in pharmaceutical R&D and manufacture has been reviewed, with the utility of the models demonstrated through two case studies based on previously published experimental data[41, 64] on the crystallisation of ibuprofen from ethanolic solution under seeded batch operating conditions. The MPB modelling, fully integrating with face-specific growth kinetics including the effect of both interface kinetics and mass transfer on the growth rates, was found to capture the crystallisation processes behaviour with the temporal evolution of the crystal shape and size distributions and also the evolution of surface areas with the respective contributions of individual faces. This was achieved by accurately quantifying the crystal shape/size and their distributions at every crystallisation time point after re-constructing the actual shape of all crystals based on the simulated individual normal distances of crystal faces and morphology information. The volume equivalent spherical diameter and crystal size distribution converted from MPB simulations were compared, for the first time, with the experimentally measured ones[64], and reasonably good agreement was reached. The new search method developed is highly applicable to industrial situation when applying the MPB approach with only limited experimental data, such as 1D volume-equivalent data, being available. It also enables the extraction of some important face-based information from the more representative volume-equivalent experimental data of a type which are generally more widely available within the pharmaceutical industry.

The development of first-principle nucleation kinetics/mechanisms and facet agglomeration and breakage kernels will involve in crystal morphology, surface chemistry, solid/solution interface, molecular modelling, hydrodynamics surrounding crystals etc. With these first-principle kinetics and kernels, MPB modelling techniques can be expected to be powerful process development tools for the digital design of the crystallisation processes used in the precision manufacture of crystals which have desirable properties including shape and size for personalised medicines. Further development of MPB with its application to crystallisation and other processes including filtration, drying, milling, blending, granulation, tableting etc. will be the planned future work.

Acknowledgments

This work was funded by the Advanced Manufacturing Supply Chain Initiative 'Advanced Digital Design of Pharmaceutical Therapeutics' (ADDoPT) project (Grant No. 14060). This work also builds upon research on morphological modelling supported by EPSRC grant 'HABIT – Crystal morphology from crystallographic and growth environment factors' through EPSRC grant EP/I028293/1 and the Synthonic Engineering programme supported by Pfizer, Boeringer-Ingellheim, Novartis and Syngenta. We also gratefully acknowledge EPSRC for the support of crystallization research at Leeds and Manchester through the Critical Mass grant 'Molecules, Clusters and Crystals' (Grant references EP/IO14446/1 and EP/IO13563/1). Finally, we gratefully acknowledge Dr D Comacho Corzo and Ms N Budesha for helpful discussions concerning the incorporation of mass transfer effects into the fitting equations for the growth rate kinetics of ibuprofen.

Conflict of interest disclosure

The authors declare no competing financial interest.

References

1. Alvarez, A. J.; Myerson, A. S., Continuous plug flow crystallization of pharmaceutical compounds. Crystal Growth & Design **2010,** 10, 2219-2228.
2. Caillet, A.; Sheibat-Othman, N.; Fevotte, G., Crystallization of monohydrate citric acid. 2. modeling through population balance equations. Crystal Growth & Design **2007,** 7, (10), 2088-2095.
3. Fevotte, G.; Alexandre, C.; Nida, S. O., A Population Balance Model of the solution-Mediated Phase Transition of citric acid. AIChE Journal **2007,** 53, (10), 2578-2589.
4. Garside, J., Industrial Crystallization from Solution. Chemical Engineering Science **1985,** 40, (1), 3-26.
5. Gerstlauer, A.; Gahn, C.; Zhou, H.; Rauls, M.; Schreiber, M., Application of population balances in the chemical industry - current status and future needs. Chemical Engineering Science **2006,** 61, (1), 205-217.
6. Hounslow, M. J.; Lewis, A. E.; Sanders, S. J.; Bondy, R., Generic crystallizer model: I. A model framework for a well-mixed compartment. AIChE Journal **2005,** 51, (11), 2942-2955.
7. Marchal, P.; David, R.; Klein, J. P.; Villermaux, J., Crystallization and precipitation engineering .1. An efficient method for solving population balance in crystallization with agglomeration. Chemical Engineering Science **1988,** 43, (1), 59-67.
8. Menon, A. R.; Kramer, H. J. M.; Grievink, J.; Jansens, P. J., Modelling the cyclic behaviour in a DTB crystallizer - a two-population blance model approach. Journal of Crystal Growth **2005,** 275, e1373-e1381.
9. Randolph, A. D.; Larson, M. A., Theory of particulate processes: Analysis and techniques of continuous crystallization. 2nd ed.; Academic Press, London: 1988.
10. Ulbert, Z.; Lakatos, B. G., Modelling and simulation of crystallisers under non-perfect micromixing conditions. Chemical Engineering Science **2005,** 60, (13), 3525-3536.
11. Ma, C. Y.; Wang, X. Z.; Roberts, K. J., Morphological population balance for modelling crystal growth in individual face directions. AIChE Journal **2008,** 54, (1), 209-222.
12. Borchert, C.; Nere, N.; Ramkrishna, D.; Voigt, A.; Sundmacher, K., On the prediction of crystal shape distributions in a steady-state continuous crystallizer Chemical Engineering Science **2009,** 64, (4), 686-696.
13. Borchert, C.; Sundmacher, K., Model Based Prediction of Crystal Shape Distributions. Computer Aided Chemical Engineering **2009,** 26, 141-146.
14. Borchert, C.; Sundmacher, K., Morphology evolution of crystal populations: Modeling and observation analysis Chemical Engineering Science **2012,** 70, 87-98.
15. Gunawan, R.; Fusman, I.; Braatz, R. D., High resolution algorithms for multidimensional population balance equations. AIChE Journal **2004,** 50, (11), 2738-2749.
16. Ma, C. Y.; Wang, X. Z., Crystal growth rate dispersion modelling using morphological population balance. AIChE Journal **2008,** 54, (9), 2321-2334.
17. Singh, M. R.; Ramkrishna, D., A Comprehensive Approach to Predicting Crystal Morphology Distributions with Population Balances. Crystal Growth & Design **2013,** 13, (3), 1397-1411.
18. Wan, J.; Wang, X. Z.; Ma, C. Y., Particle shape manipulation and optimization in cooling crystallization involving multiple crystal morphological forms. AIChE Journal **2009,** 55, (8), 2049-2061.
19. Zhang, Y. C.; Doherty, M. F., Simultaneous prediction of crystal shape and size for solution crystallization. AIChE Journal **2004,** 50, (9), 2101-2112.
20. Zhang, Y. C.; Sizemore, J. P.; Doherty, M. F., Shape evolution of 3-dimensional faceted crystals. AIChE Journal **2006,** 52, (5), 1906-1915.
21. Clydesdale, G.; Docherty, R.; Roberts, K. J., Habit - a program for predicting the morphology of molecular-crystals. Computer Physics Communications **1991,** 64, (2), 311-328.

22. Clydesdale, G.; Roberts, K. J.; Docherty, R., HABIT95 - A program for predicting the morphology of molecular crystals as a function of the growth environment. Journal of Crystal Growth **1996,** 166, (1-4), 78-83.
23. Camacho Corzo, D. M.; Ma, C. Y.; Ramachandran, V.; Roberts, K. J., Crystallisation Route Map. Springer: Dortrecht, The Neherlands, 2017; p 179-213.
24. Shaikh, L. J.; Bari, A. H.; Ranade, V. V.; Pandit, A. B., Generic Framework for Crystallization Processes Using the Population Balance Model and Its Applicability. Industrial & Engineering Chemistry Research **2015,** 54, (42), 10539–10548.
25. Liu, H.; Li, M., Two-compartmental population balance modeling of a pulsed spray fluidized bed granulation based on computational fluid dynamics (CFD) analysis. International Journal of Pharmaceutics **2014,** 475, (1-2), 256-269.
26. Aryafar, S.; Sheibat-Othman, N.; McKenna, T. F. L., Coupling of CFD Simulations and Population Balance Modeling to Predict Brownian Coagulation in an Emulsion Polymerization Reactor. Macromolecular Reaction Engineering **2017,** 11, doi.org/10.1002/mren.201600054.
27. Woo, X. Y.; Tan, R. B. H.; Braatz, R. D., Modeling and computational fluid dynamics - population balance equation - micromixing simulation of impinging jet crystallizers. Crystal Growth & Design **2009,** 9, (1), 156-164.
28. ADDoPT project www.addopt.org.
29. Wang, X. Z.; Ma, C. Y., Morphological population balance model in principal component space. AIChE Journal **2009,** 55, (9), 2370-2381.
30. Wang, X. Z.; Roberts, K. J.; Ma, C. Y., Crystal growth measurement using 2D and 3D imaging and the perspectives for shape control. Chemical Engineering Science **2008,** 63, (5), 1171-1184.
31. Ma, C. Y.; Liu, J. J.; Wang, X. Z., Measurement, modelling, and closed-loop control of crystal shape distribution: Literature review and future perspectives. Particuology **2016,** 26, 1-18.
32. Camacho, D.; Borissova, A.; Hammond, R. B.; Roberts, K. J.; Kashchiev, D.; Moore, I.; Lewtas, K., Nucleation mechanism and kinetics from the analysis of polythermal crystallisation data: methyl stearate from kerosene solutions. CrystEngComm **2014,** 16, 974-991.
33. Nyvlt, J., Kinetics of nucleation in solutions. Jornal of Crystal Growth **1968,** 4, 377-383.
34. Nyvlt, J.; Rychly, R.; Gottfried, J.; Wurzelova, J., Metastable Zone Width of some aqueous solutions. Jornal of Crystal Growth **1970,** 6, 151-162.
35. Kashchiev, D.; Borissova, A.; Hammond, R. B.; Roberts, K. J., Effect of cooling rate on the critical undercooling for crystallization. Journal of Crystal Growth **2010,** 312, 698-704.
36. Kashchiev, D.; Borissova, A.; Hammond, R. B.; Roberts, K. J., Dependence of the Critical Undercooling for Crystallization on the Cooling Rate. Journal of Physical Chemistry B **2010,** 114, 5441-5446.
37. Shiau, L.-D.; Lu, Y.-F., Modeling solute clustering in the diffusion layer around a growing crystal. Journal of Chemical Physics **2009,** 130, (094105).
38. Kitamura, M.; Hayashi, Y., Secondary Nucleation Behavior and the Mechanism in Antisolvent Crystallization of Thiazole Derivative Polymorphs. Industrial & Engineering Chemistry Research **2016,** 55, (5), 1413-1418.
39. Burton, W. K.; Cabrera, N.; Frank, F. C., The growth of crystals and the equilibrium structure of their surfaces. Philosophical Transactions of the Royal Society of London **1951,** 243, 299-358.
40. Weeks, J. D.; Gilmer, G. H., Dynamics of crystal growth. Advances in Chemical Physics **1979,** 40, 157-227.
41. Nguyen, T. T. H.; Hammond, R. B.; Roberts, K. J.; Marziano, I.; Nichols, G., Precision measurement of the growth rate and mechanism of ibuprofen {001} and {011} as a function of crystallization environment. CrystEngComm **2014,** 16, 4568-4586.
42. Nguyen, T. T. H. Influence of crystallisation environment on the nucleation and growth of single crystals of (RS)-ibuprofen, PhD Thesis. University of Leeds, 2013.
43. Ochsenbein, D. R.; Vetter, T.; Morari, M.; Mazzotti, M., Agglomeration of Needle-like Crystals in Suspension. II. Modeling. Crystal Growth & Design **2015,** 15, 4296-4310.

44. Eisenschmidt, H.; Soumayaa, M.; Bajcincab, N.; S., L. B.; Sundmacher, K., Estimation of aggregation kernels based on Laurent polynomial approximation. Computers & Chemical Engineering **2017,** 103, (4), 210–217.
45. Grof, Z.; Schoellhammer, C. M.; Rajniak, P.; Stepánek, F., Computational and experimental investigation of needle-shaped crystal breakage. International Journal of Pharmaceutics **2011,** 407, 12-20.
46. Ramkrishna, D.; Mahoney, A. W., Population balance modeling. Promise for the future. Chemical Engineering Science **2002,** 57, (4), 595-606.
47. Omar, H. M.; Rohani, S., Crystal Population Balance Formulation and Solution Methods: A Review. Crystal Growth & Design **2017,** 17, 4028-4041.
48. Briesen, H., Two-dimensional population balance modeling for shape dependent crystal attrition. Chemical Engineering Science **2009,** 64, (4), 661-672.
49. Ma, C. Y.; Wang, X. Z.; Roberts, K. J., Multi-dimensional population balance modelling of the growth of rod-like L-glutamic acid crystals using growth rates estimated from in-process imaging. Advanced Powder Technology **2007,** 18, (6), 707-723.
50. Oullion, M.; Puel, F.; Fevotte, G.; Righini, S.; Carvin, P., Industrial batch crystallization of a plate-like organic product. In situ monitoring and 2D-CSD modelling. Part 2: Kinetic modelling and identification. Chemical Engineering Science **2007,** 62, (3), 833-845.
51. Puel, F.; Fevotte, G.; Klein, J. P., Simulation and analysis of industrial crystallization processes through multidimensional population balance equations. Part 1: a resolution algorithm based on the method of classes. Chemical Engineering Science **2003,** 58, (16), 3715-3727.
52. Puel, F.; Fevotte, G.; Klein, J. P., Simulation and analysis of industrial crystallization processes through multidimensional population balance equations. Part 2: a study of semi-batch crystallization. Chemical Engineering Science **2003,** 58, (16), 3729-3740.
53. Sato, K.; Nagai, H.; Hasegawa, K.; Tomori, K.; Kramer, H. J. M.; Jansens, P. J., Two-dimensional population balance model with breakage of high aspect ratio crystals for batch crystallization. Chemical Engineering Science **2008,** 63, (12), 3271-3278.
54. Shi, D.; El-Farra, N. H.; Li, M.; Mhaskar, P.; Christofides, P. D., Predictive control of particle size distribution in particulate processes. Chemical Engineering Science **2006,** 61, (1), 268-281.
55. Liu, J. J.; Hu, Y. D.; Wang, X. Z., Optimisation and control of crystal shape and size in protein crystallisation process. Computers and Chemical Engineering **2013,** 57, 133-140.
56. Liu, J. J.; Ma, C. Y.; Hu, Y. D.; Wang, X. Z., Modelling protein crystallisation using morphological population balance models. Chemical Engineering Research & Design **2010,** 88, (4), 437-446.
57. Liu, J. J.; Ma, C. Y.; Hu, Y. D.; Wang, X. Z., Effect of seed loading and cooling rate on crystal size and shape distributions in protein crystallization—A study using morphological population balance simulation. Computers and Chemical Engineering **2010,** 34, (12), 1945-1952.
58. Ma, C. Y.; Wang, X. Z., Model identification of crystal facet growth kinetics in morphological population balance modeling of L-glutamic acid crystallization and experimental validation. Chemical Engineering Science **2012,** 70, 22-30.
59. Chakraborty, J.; Singh, M. R.; Ramkrishna, D.; Borchert, C.; Sundmacher, K., Modeling of crystal morphology distributions. Towards crystals with preferred asymmetry. Chemical Engineering Science **2010,** 65, 5676-5686.
60. Borchert, C.; Sundmacher, K., Efficient formulation of crystal shape evolution equations. Chemical Engineering Science **2012,** 84, 85-99.
61. Kwon, J. S.; Nayhouse, M.; Christofides, P. D.; Orkoulas, G., Modeling and control of protein crystal shape and size in batch crystallization. AIChE Journal **2013,** 59, 2317-2327.
62. Kwon, J. S.; Nayhouse, M.; Christofides, P. D.; Orkoulas, G., Modeling and control of crystal shape in continuous protein crystallisation. Chemical Engineering Science **2014,** 107, 47-57.
63. Majumder, A.; Nagy, Z. K., Prediction and control of crystal shape distribution in the presence of crystal growth modifiers Chemical Engineering Science **2013,** 101 593-602.

64. Rashid, A.; White, E.; Howes, T.; Litster, J.; Marziano, I., Growth rates of ibuprofen crystals grown from ethanol and aqueous ethanol. Chemical Engineering Research & Design **2012,** 90, 158-161.
65. Rashid, A.; White, E.; Howes, T.; Litster, J.; Marziano, I., From Raw Data to Process: The Path to a Batch or a Continuous Crystallizer Design for Ibuprofen. Organic Process Research & Development **2017,** 21, 187-194.
66. Nguyen, T. T. H.; Rosbottom, I.; Marziano, I.; Hammond, R. B.; Roberts, K. J., Crystal Morphology and Interfacial Stability of RS-Ibuprofen in Relation to Its Molecular and Synthonic Structure. Cryst. Growth Des. **2017,** 17, (6), 3088–3099.
67. Camacho, D. M.; Roberts, K. J.; Muller, F.; Thomas, D.; More, I.; Lewtas, K., Morphology and Growth of Methyl Stearate as a Function of Crystallization Environment. Crystal Growth & Design **2016,** 17, (563−575), 2088-2095.
68. Pinto, M. A.; Immanuel, C. D.; Doyle III, F. J., A feasible solution technique for higher-dimensional population balance models. Computers & Chemical Engineering **2007,** 31, 1242-1256.
69. Attarakih, M. M.; Drumm, C.; Bart, H., Solution of the population balance equation using the sectional quadrature method of moments (SQMOM). Chemical Engineering Science **2009,** 64, 742-752.
70. Shampine, L. F.; Watts, H. A. In Subroutine RKF45, Computer Methods for Mathematical Computations, Englewood Cliffs, N. J., 1977; G. E. Forsythe, M. A. M., C. B. Moler, Ed. Prentice-Hall: Englewood Cliffs, N. J., 1977; pp 135-147.
71. Nayhouse, M.; Tran, A.; Kwon, J. S.; Crose, M.; Orkoulas, G.; Christofides, P. D., Modeling and control of ibuprofen crystal growth and size distribution. Chemical Engineering Science **2015,** 134, 414-422.